A new Sun: Probing solar plasmas in the extreme-ultraviolet light from SUMER on *SOHO*

Bhola N. Dwivedi*,,†, Anita Mohan* and Klaus Wilhelm****

*Department of Applied Physics, Institute of Technology, Banaras Hindu University, Varanasi 221 005, India
**Max-Planck-Institut für Aeronomie, 37191 Katlenburg-Lindau, Germany

We briefly outline the extreme-ultraviolet spectroscopy of solar plasmas in the light of a wealth of high-resolution observations, both in spectral and spatial regimes, from the SUMER spectrograph (Solar Ultraviolet Measurements of Emitted Radiation) on the spacecraft *SOHO* (Solar and Heliospheric Observatory). We then present some of the new results on a new Sun seen by the SUMER spectrograph. In particular, we discuss coronal holes and the solar wind, the 'red'/'blue' Sun, abundance anomalies, explosive events and sunspot transition region oscillations. We conclude this article by reiterating clues, obtained from SUMER, that provide information essential for solving solar riddles of coronal heating and the wind acceleration.

Introduction

THE Sun presents us with a thousand-fold face. Depending on the ways we observe it, whether it be through a ground-based telescope, during an eclipse, or from a space observatory, we see a different Sun. One can distinguish the wavelengths in which it is observed: X-rays, ultraviolet, visible, infrared, radio or even by non-photon instruments (e.g. neutrino detectors). One can distinguish the time when it is observed: near the maximum activity of its sunspot cycle, or the minimum activity. Still this multi-faceted Sun of ours is a single celestial object, and it is this idea of the Sun as whole that has been described in the previous articles of this special issue. A new Sun that has emerged from the analysis and the interpretation of observations from the Solar Ultraviolet Measurements of Emitted Radiation (SUMER) spectrograph is briefly presented in this article.

Full descriptions of the SUMER spectrograph on the spacecraft *SOHO* and its performance are available[1-3]. Briefly, the SUMER spectrograph observes the Sun in the extreme-ultraviolet (EUV) light from 465 Å to 1610 Å with high spatial and spectral resolution. This wavelength range contains EUV lines from the chromosphere, the transition region, and the corona, thereby providing a unique opportunity to probe plasmas of the solar atmosphere. The spatial resolution is close to 1″ (about 715 km at the Sun), while the spectral resolution element (one pixel) is about 44 mÅ in first order of diffraction and 22 mÅ in second order. The spectral resolution, which can be improved for relative (and under certain conditions for absolute) measurements to fractions of a pixel, allows to measure Doppler shifts corresponding to plasma bulk velocities of about 1 km s^{-1} along the line of sight. Turbulent velocities are obtained by determining line broadenings. Vast literature has resulted on the basis of observations carried out using SUMER. But, we have not reviewed this in the present article. Instead, we present some new results from SUMER on solar plasmas that have added a new dimension to a better understanding of some of the solar mysteries, especially coronal heating and the solar wind acceleration.

Plasma diagnostics

Without a knowledge of the densities, temperatures, and elemental abundances of space plasmas, almost nothing can be said regarding the generation and transport of mass, momentum and energy. Thus, since early in the era of space-borne spectroscopy we have faced the task of inferring plasma temperatures, densities, and elemental abundances for hot solar and other astrophysical plasmas from optically thin emission-line spectra[4,5]. A fundamental property of hot solar plasmas is their inhomogeneity. The emergent intensities of spectral lines from optically thin plasmas are determined by integrals along the line of sight (*LOS*) through the plasma. Spectroscopic diagnostics of the temperature and density structures of hot optically thin plasmas using emission-line intensities is usually described in two ways. The simplest approach, the line-ratio diagnostics, uses an observed line-intensity ratio to determine density or temperature from theoretical density or temperature-sensitive line-ratio curves, based on an atomic model and taking account of physical processes for the formation of lines. The line-ratio method is stable, leading to well-defined values of T_e or N_e, but in realistic cases of inhomogeneous plasmas these are hard to interpret, since each line pair yields a different value of density or temperature. The more general differential emission measure (DEM) method recognizes that obser-

†For correspondence. (e-mail: dwivedi@banaras.ernet.in)

ved plasmas are better described by distributions of temperature or density along the *LOS*, and poses the problem in inverse form. It is well known that the DEM function is the solution to the inverse problem, which is function of T_e, N_e, or both. Derivation of DEM functions, while more generally acceptable, is unstable to noise and errors in spectral and atomic data. The exact relationship between the two approaches has never been explored in depth, although particular situations were discussed[6]. The mathematical relationship between these two approaches has recently been reported[7].

Line shifts and broadenings give information about the dynamic nature of the solar and stellar atmospheres. The transition region spectra from the solar atmosphere are characterized by broadened line profiles. The nature of this excess broadening puts constraints on possible heating processes. Systematic redshifts in transition region lines have been observed in both solar spectra and stellar spectra of late-type stars. On the Sun, outflows of coronal material have been correlated with coronal holes. The excess broadening of coronal lines above the limb provides information on wave propagation in the solar wind. Figure 1 shows the full Sun raster image obtained by SUMER in the Ne VIII (λ770) line on 2 February 1996. The emission line is formed at 630000 K and observed in second order. The polar coronal holes are clearly seen in this line as well as some bright points and polar plumes[8]. In Figure 2 a Doppler velocity map is shown, derived from the Ne VIII observations under the assumption that the line shifts can be interpreted as plasma flows. The range of the velocity scale is from -30 km s^{-1} (blue) to $+30$ km s^{-1} (red). The zero point is adjusted to give no Doppler shift just above the limb at about 20 arc sec. The blue polar coronal holes stand out with some white spots, which upon close inspection, coincide with bright points in the intensity image. Strong up and down motions can be seen near the active regions in the western hemisphere.

Coronal holes and the solar wind

In 1950s Waldmeier[9] first recognized persistent depressions in the intensity of the monochromatic corona (outside the polar caps) as observed by ground-based coronagraphs and called them 'holes' (Löcher in German). He published his coronal observations obtained between 1939 and 1952 (during the solar cycles 17 and 18). At the end of cycle 17, coronal holes were identified in coronal maps. More than 20 years later, after theoretical predictions, Krieger *et al.*[10] related a coronal hole, seen on

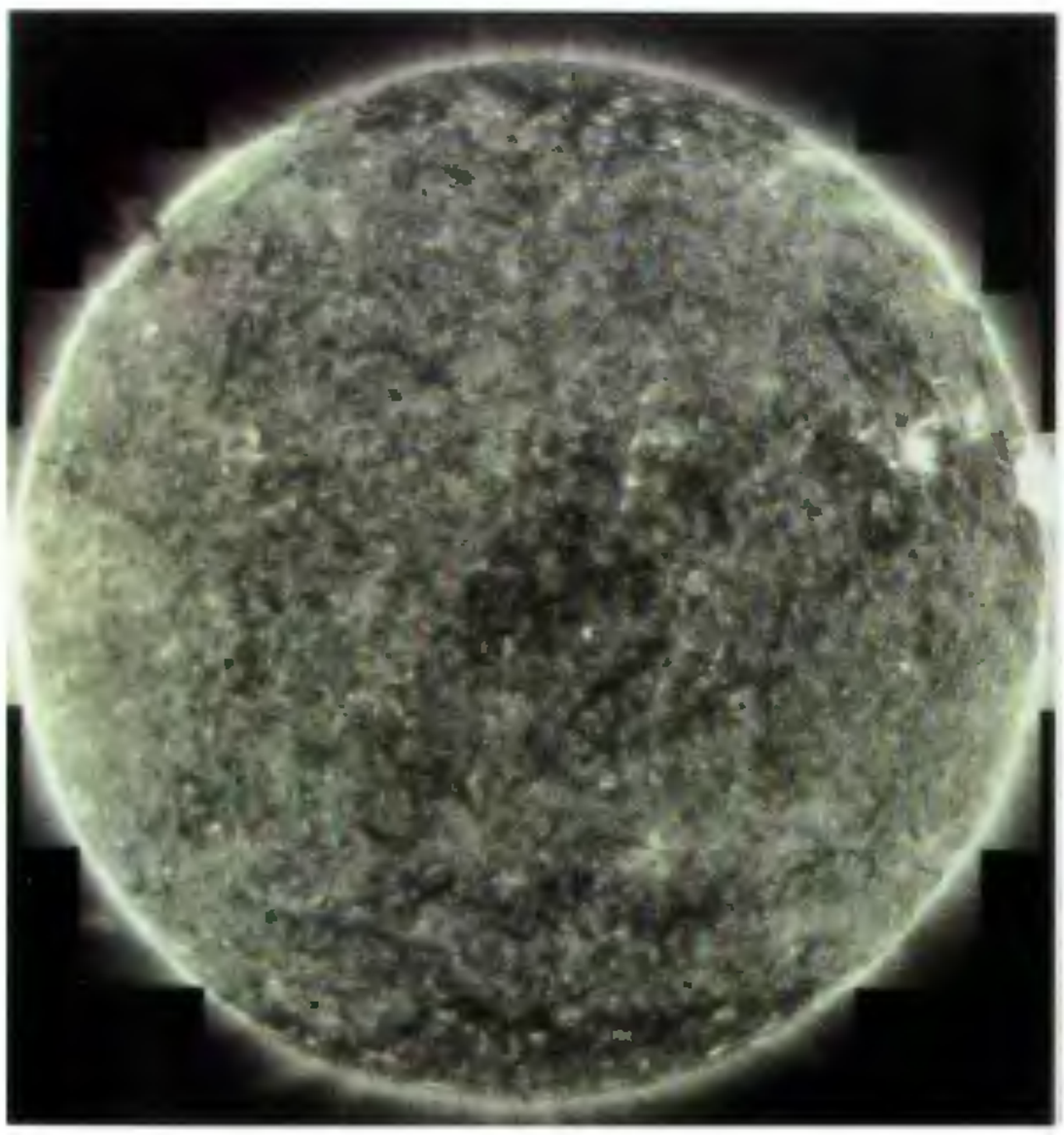

Figure 1. Full Sun raster image obtained by Solar Ultraviolet Measurements of Emitted Radiation (SUMER) in the line Ne VIII (λ770) on 2 February 1996. The emission line is formed at a temperature of 630000 K and observed in second order of diffraction on the bare microchannel plate portion of detector A. The 1″ x 300″ slit was used with a step width of 1.88″ and an exposure time of 7.5 s. The polar coronal holes can clearly be seen in this line as well as some bright points and polar plumes (from Wilhelm *et al.*[8]).

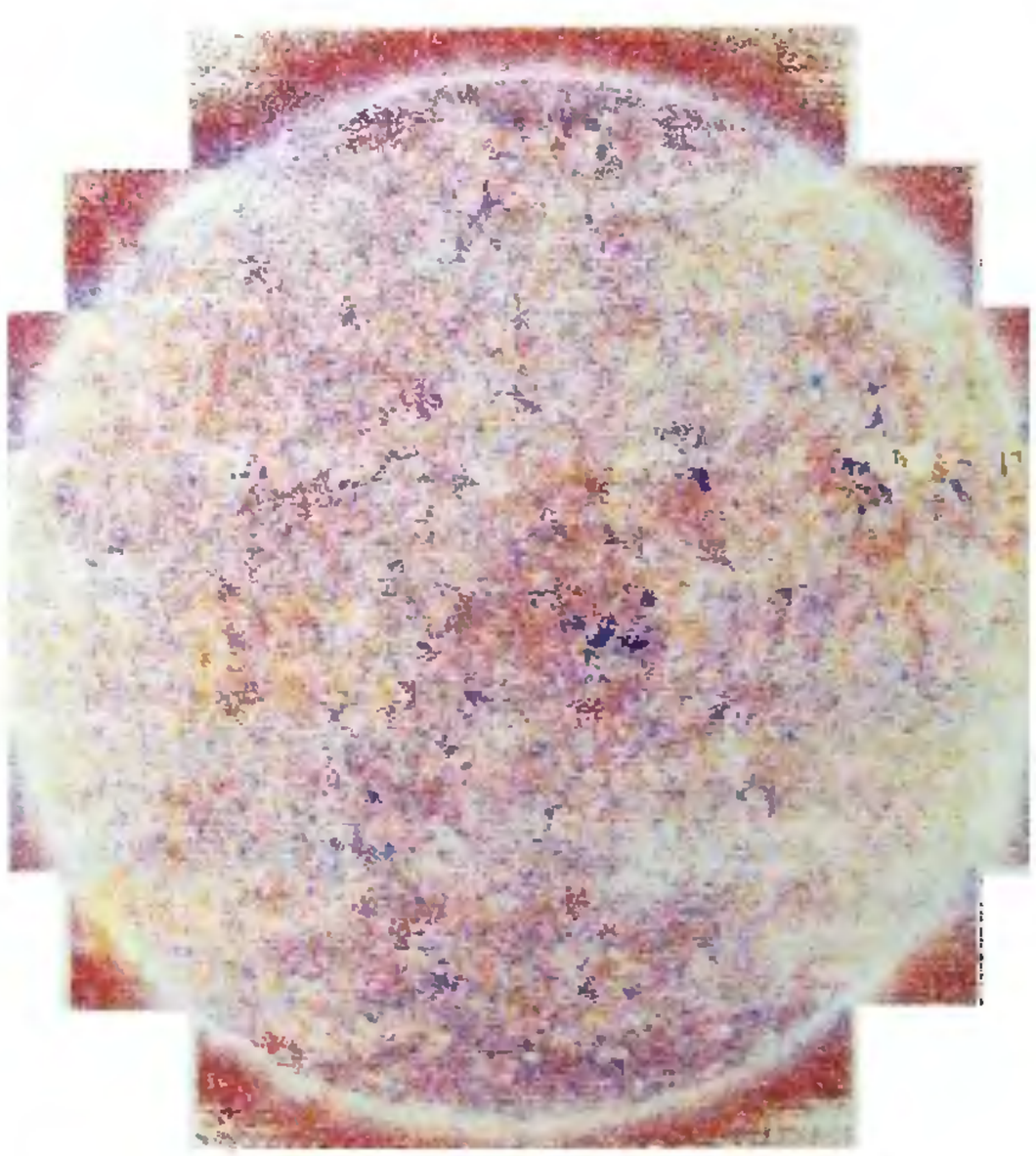

Figure 2. Doppler velocity map derived from the Ne VIII observations shown in Figure 1. The range of the velocity scale from -30 km s^{-1} (blue) to $+30$ km s^{-1} (red). The zero point is adjusted to give no Doppler shift just above the limb (at ~20″). The blue polar coronal holes stand out with some white spots, which upon close inspection, coincide with bright points in the intensity image. Strong up and down motions can be seen near the active regions in the western hemisphere.

an X-ray image taken on 24 November 1970 during a sounding rocket flight, to a recurrent high-speed stream of the solar wind observed by instruments on PIONEER-VI and on the Vela satellite.

Observations from the Skylab mission further established that the high-speed solar wind originates in coronal holes which are well-defined regions of strongly reduced EUV and soft X-ray emissions[11]. More recent data from Ulysses show the importance of the polar coronal holes, particularly at times near the solar minimum when a magnetic dipole dominates the field configuration. Figure 3 shows a polar coronal hole with bright points and polar plumes[12] seen in Mg X (λ625) with a formation temperature of ~ 1100000 K. The mechanism for accelerating the wind to the high values observed, of the order of 800 km s^{-1}, is not understood quantitatively. The Parker model[13] is based upon a thermally driven wind. To reach such high velocities, temperatures of the order 3 to 4 MK would be required near the base of the corona. However, other processes are available for acceleration of the wind, for example the direct transfer of momentum from magneto-hydrodynamic (MHD) waves, with or without dissipation. This process results from the decrease of momentum of the waves as they enter less dense regions, coupled with the need to conserve momentum of a system consisting of waves plus the local plasma. If this transfer predominates, it may not be necessary to invoke high coronal temperatures at the base of the corona.

In reality, very little information was available on the density and temperature structure in coronal holes prior to the *SOHO* Mission. Data from Skylab is limited, due to the very low intensities in holes and the poor spectral resolution, leading to many line blends. Skylab was able to follow temperatures up to nearly 1 MK and no further, and the interpretation of the data is quite uncertain. High-resolution EUV observations from instruments on *SOHO* provided the opportunity to infer the density and temperature profile in coronal holes. Wilhelm *et al.*[14] observed several polar coronal holes with SUMER spectrograph in Si VIII lines at 1445.75 Å and 1440.49 Å and Mg IX lines at 706 Å and 750 Å to determine density and temperature structure via line-ratio spectroscopic diagnostics. Figure 4 shows the electron densities deduced. Comparing the electron temperatures with the ion temperatures, Wilhelm *et al.* concluded that ions are extremely hot and the electrons are relatively cool. This result is also in agreement with the UVCS (Ultraviolet Coronagraph Spectrometer) *SOHO* results[15] at greater altitudes.

Using the two *SOHO* instruments CDS (Coronal Diagnostic Spectrometer) and SUMER David *et al.*[16] have now measured electron temperatures as a function of height above the limb in a polar coronal hole. Observations of two lines from the same ion stage O VI 1032 Å from SUMER and O VI 173 Å from CDS/*SOHO* were made to determine the electron temperature gradient in a coronal hole. They deduced temperatures of around 0.8 MK close to the limb, rising to a maximum of less than 1 MK at 1.15 $R_\odot$, then falling to around 0.4 MK at 1.3 $R_\odot$. It seems that present observations preclude the existence of temperatures over 1 MK at any height near the centre of a coronal hole. Wind acceleration by temperature effects is therefore inadequate as an explanation of the high-speed wind and it becomes essential to look towards other effects, probably involving the momentum and the energy of Alfvén waves.

The 'red'/'blue' Sun

In the so-called transition region, the temperature rises sharply from some 10000 K to more than 1 MK. It has been known since the Skylab period that there is a net red shift in the transition region lines[17]. It has recently been reported that the redshift peaks at about 12 km s^{-1} near 150000 K and extends into the hotter regions where Ne VIII emission line is formed[18,19]. Ne VIII belongs to the

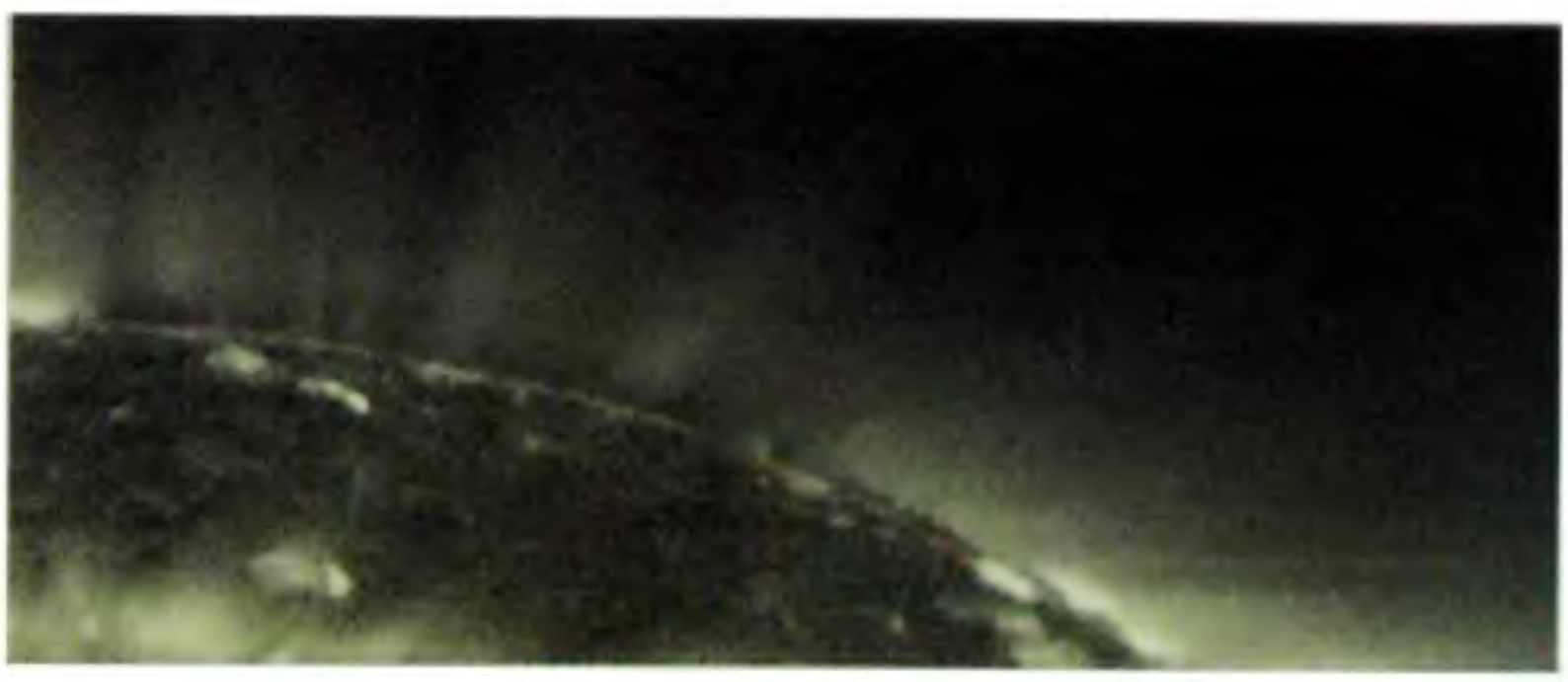

Figure 3. Polar coronal hole with bright points and polar plumes seen in Mg X (λ625) with a formation temperature of ~ 1100000 K (from Dammasch *et al.*[12]).

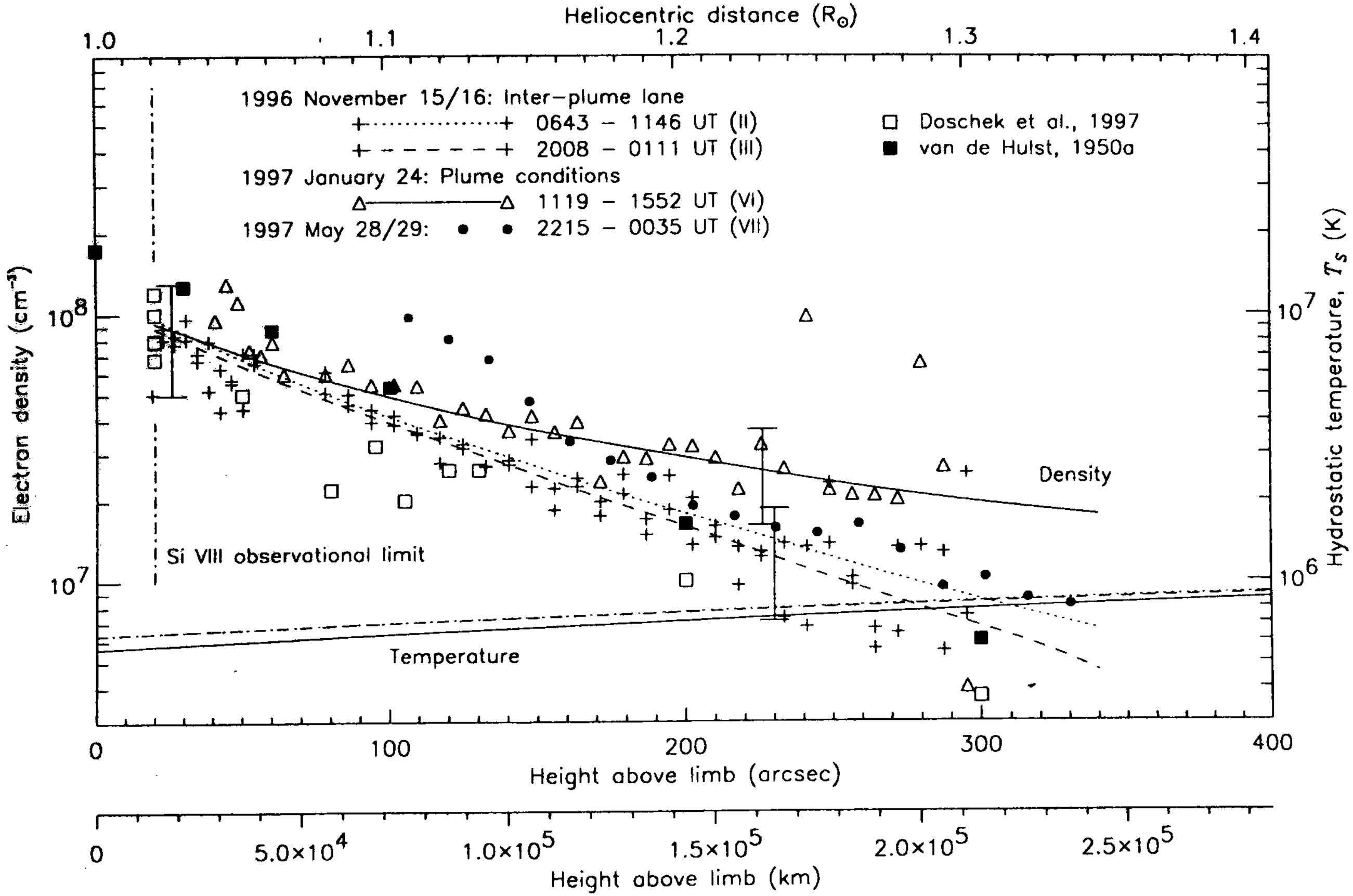

Figure 4. Electron densities derived from our Si VIII line ratios and a comparison with data in literature. The hydrostatic temperature, T_s, used for the fits of the line height profile of Si VIII (λ1445) is plotted in the lower portion of the diagram with a scale on the right-hand side. The points labelled "28/29 May 1997" are obtained from line ratios observed west of the polar plume assembly in a very dark region of the corona (for data points above 1.2×10^5 km). The uncertainty margins indicate a density variation resulting from a ± 30% uncertainty in the line ratio determination. Note that there is a small (< 3%) seasonal variation between the angular and the spatial scales for different data set (from Wilhelm *et al.*[14]).

Li-sequence and has a strong $2s$–$2p$ resonance line at 770 Å which is observed by SUMER in both first- and second-order. A laboratory wavelength of (770.409 ± 0.005) Å was used for this line. Dammasch *et al.*[20] made an accurate wavelength measurement of this line recorded in second order together with several S I and C I lines, which have well-known wavelengths. Assuming that there is no net Doppler flow along the line of sight at and above the limb and eliminating other residual errors, a rest wavelength of (770.428 ± 0.003) Å was derived. With 1 mÅ corresponding to 390 m s^{-1}, this new result moves the Doppler shift of Ne VIII towards the blue by (–)7.4 km s^{-1}. This immediately implies that there is no net downflow at this temperature in quiet Sun regions.

That the solar wind is coming from coronal holes (open magnetic field regions in the corona) has been widely accepted, although little additional direct observational evidence has been obtained to support this view. Hassler *et al.*[21] found the Ne VIII emission blueshifted in the north polar coronal hole along the magnetic network boundary and at network boundary interfaces compared to the average quiet Sun flow. We show in Figure 5 velocity map of the Ne VIII (λ770) line as observed on 21 September 1996 (top panel). The areas of dark blue, corresponding to an outflow velocity of more than 5 km s^{-1} (*LOS*), are enriched by contours. A repeat of the velocity contours is overlaid on the intensity diagram of the same area in the bottom panel. It is to be noted that coronal hole conditions prevail in the northern portion of the field of view (520″ × 300″), whereas quiet Sun regions are present in the south. These Ne VIII observations reveal the first two-dimensional coronal images showing velocity structure in a coronal hole, and provide strong evidence that coronal holes are indeed the source of the fast solar wind. The apparent relationship to the chromospheric magnetic network, as well as the relatively large outflow velocity signatures at the intersections of network boundaries at midlatitudes, is a first step in better understanding the complex structure and dynamics at the base of the corona and the source region of the solar wind.

Abundance anomalies

The status of coronal abundances relative to hydrogen is not entirely settled. It is often suggested that abundances are correlated with the first ionization potential (FIP). Many studies show that 'FIP bias' does exist[22–24]. Classically, a step function increase by a factor of 4 is assumed for elements with increasing FIP. The FIP effect should eventually offer valuable clues to the process of heating, ionization, and injection of material into coronal and flaring loops for the Sun and other stars.

Dwivedi *et al.*[25] presented results from a study of EUV off-limb spectra obtained on 20 June 1996 with SUMER spectrograph. They recorded Ne VI and Mg VI inter-combination/forbidden lines, which provided good possibilities to study the relative element abundance of Ne (high FIP) and Mg (low FIP) in transition region emission in the corona. The observation of the FIP effect in transition region emission in the corona is a new observational fact. Laming *et al.*[26] have also investigated the behaviour of the FIP effect with height above the solar limb in a region of diffuse quiet corona and found a low FIP bias of a factor of 3 to 4, with no significant height variation. Yet another study confirmed the new observational facts about FIP effects in transition region emission[27] which is shown in Figure 6 for the Mg/Ne FIP bias from four line ratios as a function of height above the limb.

Explosive events

The universe abounds with explosive energy release that may heat plasma to millions of degrees and accelerate

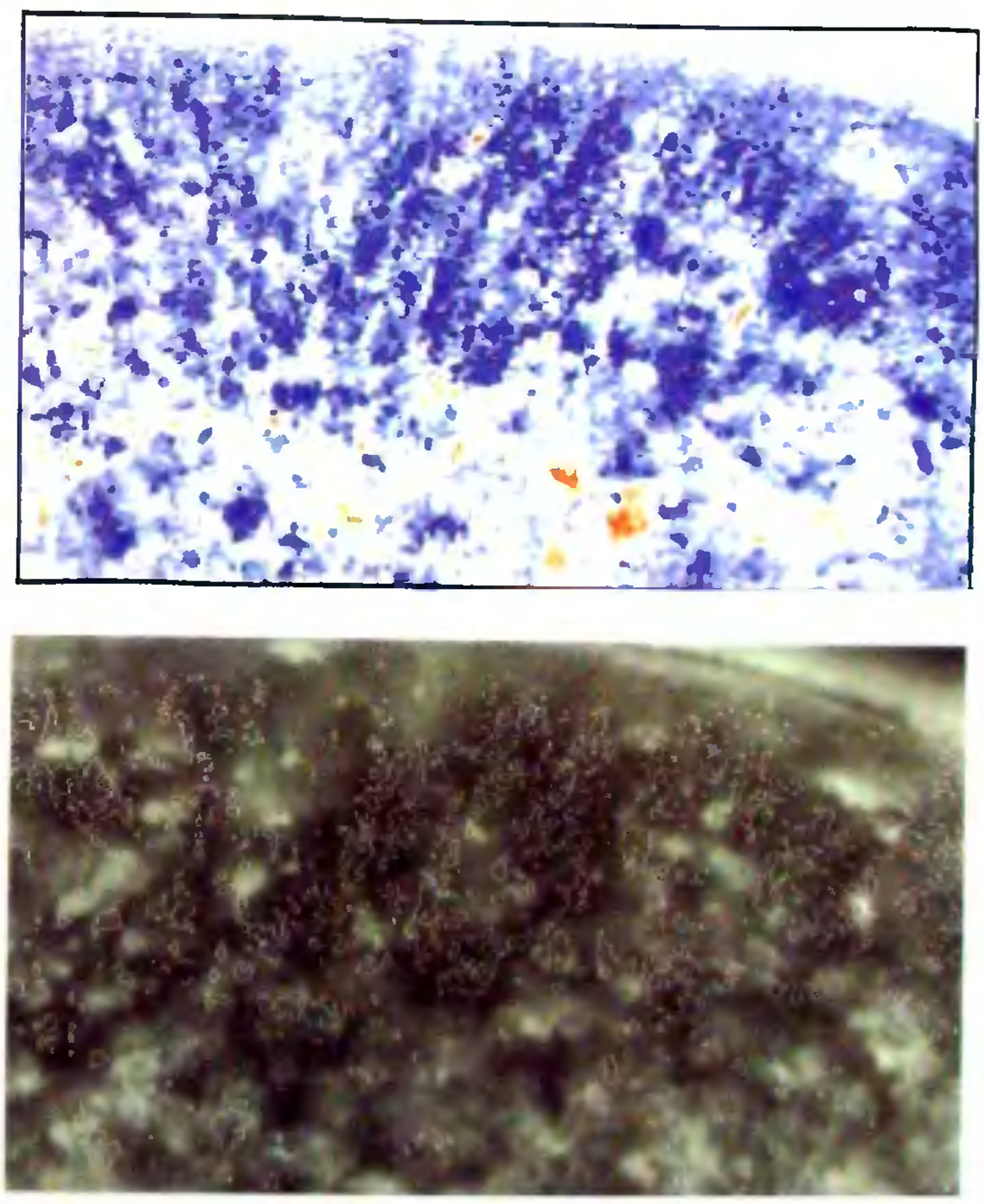

Figure 5. Velocity map of the Ne VIII (λ770) line as observed on 21 September 1996 (top panel). The areas of dark blue, corresponding to an outflow velocity of more than 5 km s^{-1} *LOS* (line-of-sight), are enriched by contours. Single pixel contributions have been eliminated by a floating average over 3″ in east–west and north–south directions. A repeat of the velocity contours is overlaid on the intensity diagram of the same area in the bottom panel. Note that coronal hole conditions prevail in the northern portion of the field of view (520″ × 300″), whereas quiet Sun regions are present in the south.

particles to relativistic velocities. Such occurrences are not uncommon on our own star too. Examples include solar flares, coronal mass ejections, chromospheric and coronal microflares, etc. In many cases, the magnetic field seems to be the only source of energy available to power these cosmic explosions. While it is well established that the Sun has a large reservoir of magnetic energy, the reason for its release is still debated.

The widely accepted explanation for explosive energy release is a process known as magnetic reconnection. This effectively involves the cutting and reattachment of magnetic lines of force. Many solar physicists feel that reconnection is observationally and theoretically well established. Sceptics, however, argue that there is no definite proof for the reconnection taking place on the Sun. It is for this reason that new results from SUMER for the magnetic reconnection on the Sun is so important. They provide the best evidence to date for the existence of bi-directional outflow jets, forming fundamental part of the standard reconnection model.

Explosive events[28] were first seen in the ultraviolet spectra obtained with the NRL's (Naval Research Laboratory) High Resolution Telescope and Spectrograph (HRTS) flown on several rocket flights and Spacelab 2. They were found to be short-lived (60 sec), small-scale (1500 km), high-velocity ($\pm$ 150 km s^{-1}) flows that occurred very frequently over the entire surface of the Sun. There are estimated to be 30,000 events at any one time on the Sun. The energy involved in the events observed, however, suggests that they are not the major source of mass or energy in either chromosphere or corona. Their importance lies in the fact that they probably represent the high energy tail of a spectrum of network events that occur on scales unobservable with current techniques. It is also noted that explosive events are associated with freshly emerged magnetic field and their Doppler velocities are roughly equal to the Alfvén speed in the chromosphere. The suggestion is that the events result from magnetic reconnection. Possible evidence for bi-directional nature of the flows had been noted in earlier spectroscopic data but the examples were not very clear. This was so because the structure of the flow could not be resolved due to limited time and space coverage by previous space experiments.

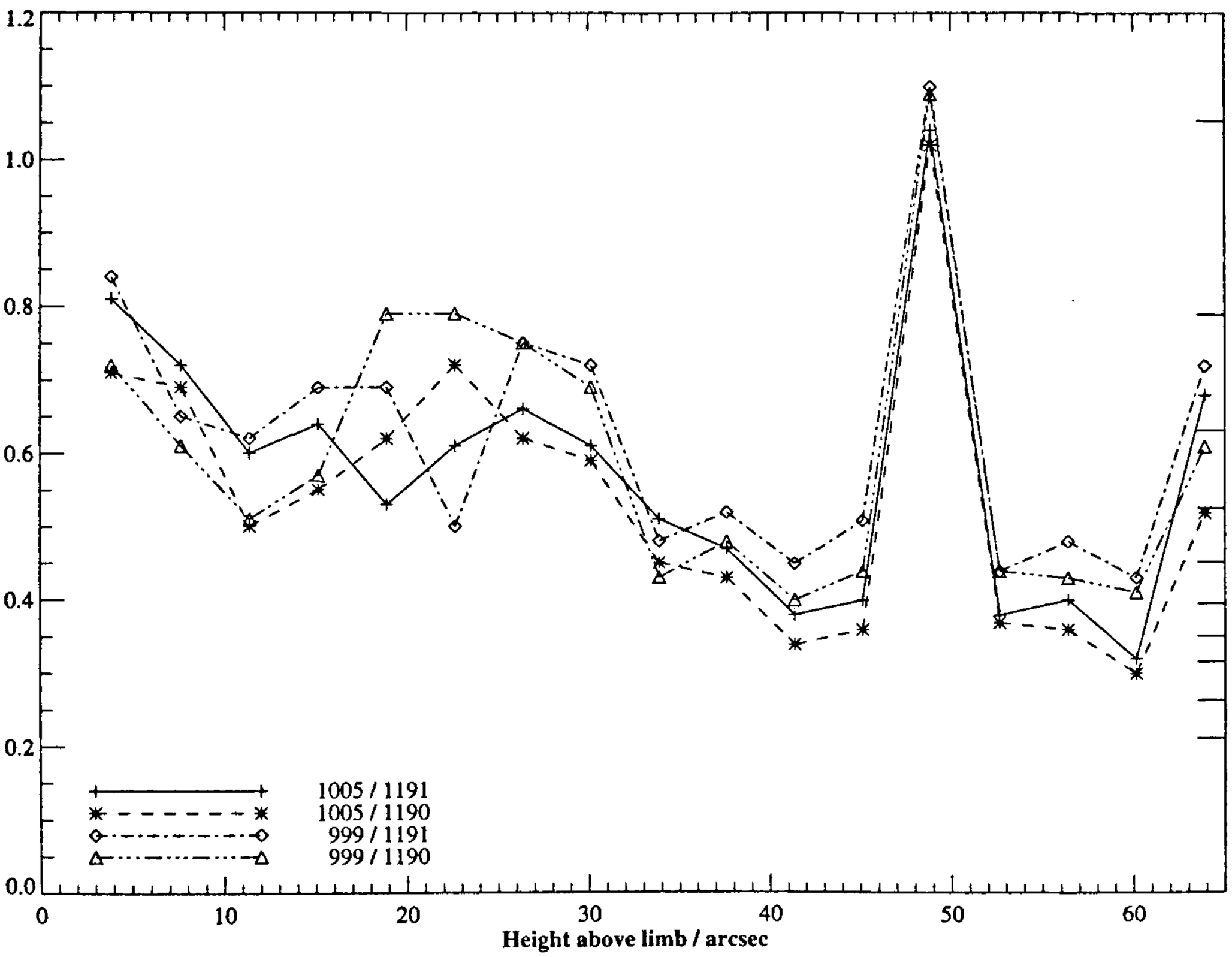

Figure 6. Mg/Ne FIP bias derived from four line ratios as a function of height above the limb (from Dwivedi *et al.*[27]).

The SUMER spectrograph has now made it possible to observe the chromospheric network continuously over an extended period and to discern the spatial structure of the flows associated with these explosive events. The observation that explosive events are bi-directional jets, provides new evidence that they result from magnetic reconnection above the solar surface. From simultaneous magnetic field and ultraviolet measurements, it has already been suggested that explosive events are often found on the chromospheric network boundary and seem to be associated with the cancellation of photospheric magnetic fields. The network consists of curtains of very strong magnetic flux tubes. All flux tubes are anchored by their footpoints to the photosphere. The continual motions in the photosphere mean that field lines of opposite-polarity are naturally drawn together. If flux tubes with opposite-polarity field lines are pushed together, a current sheet forms. In a finite resistivity plasma, a small region near the neutral region may collapse and create a thin reconnection region. From this region, plasma is ejected in both directions along the field lines, with velocity of the order of the Alfvén speed (the Alfvén speed depends on magnetic field strength and plasma density). Electrical resistance to this current flow liberates energy from the system to heat the plasma, much in the same way as the filament of a light bulb is heated.

Interpreting the evolution of the jets in the Si IV 1393 Å line profile, Innes *et al.*[29] have now shown that explosive events have the bi-directional jets ejected from small sites above the solar surface. In Figure 7, we show the explosive events seen in the Si IV (λ1393) line. The SUMER spectrograph slit shown in each section has a projected length of 84000 km on the Sun and a width of 700 km. The exposure time was 10 s each. The Doppler shift near bright portions correspond to plasma motions with line-of-sight velocities ± 150 km s^{-1}. The structure of these plasma jets evolves in the manner predicted by theoretical models of magnetic reconnection. This lends support to the view that magnetic reconnection is one of the fundamental processes for accelerating plasma on the

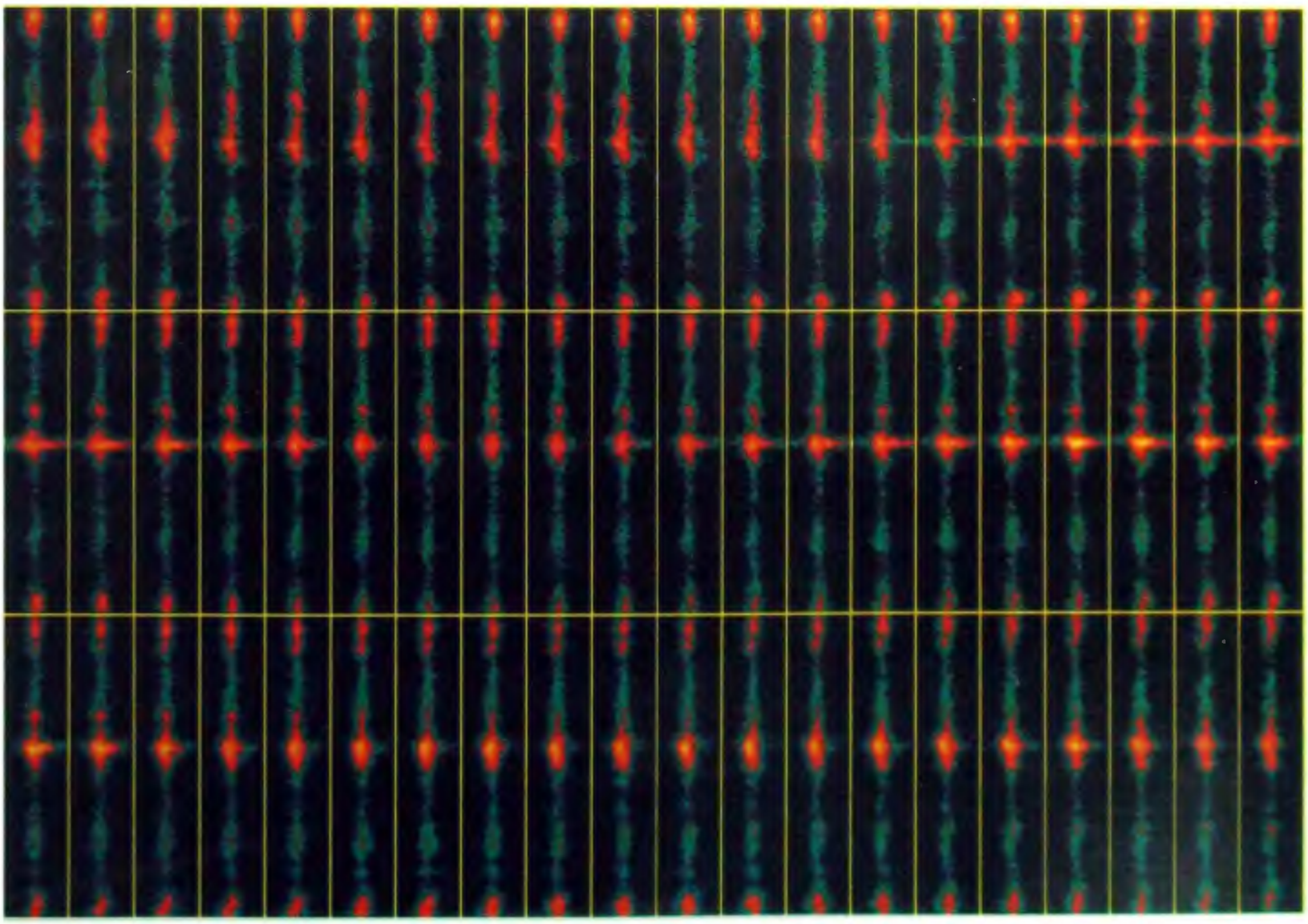

Figure 7. Explosive events seen in the Si IV (λ1393) line. The SUMER spectrograph slit shown in each section has a projected length of 84000 km on the Sun and a width of 700 km. The exposure time was 10 s each. The Doppler shift near bright portions (i.e. at chromospheric network crossings of the slit) correspond to plasma motions with line-of-sight velocities ± 150 km s^{-1}

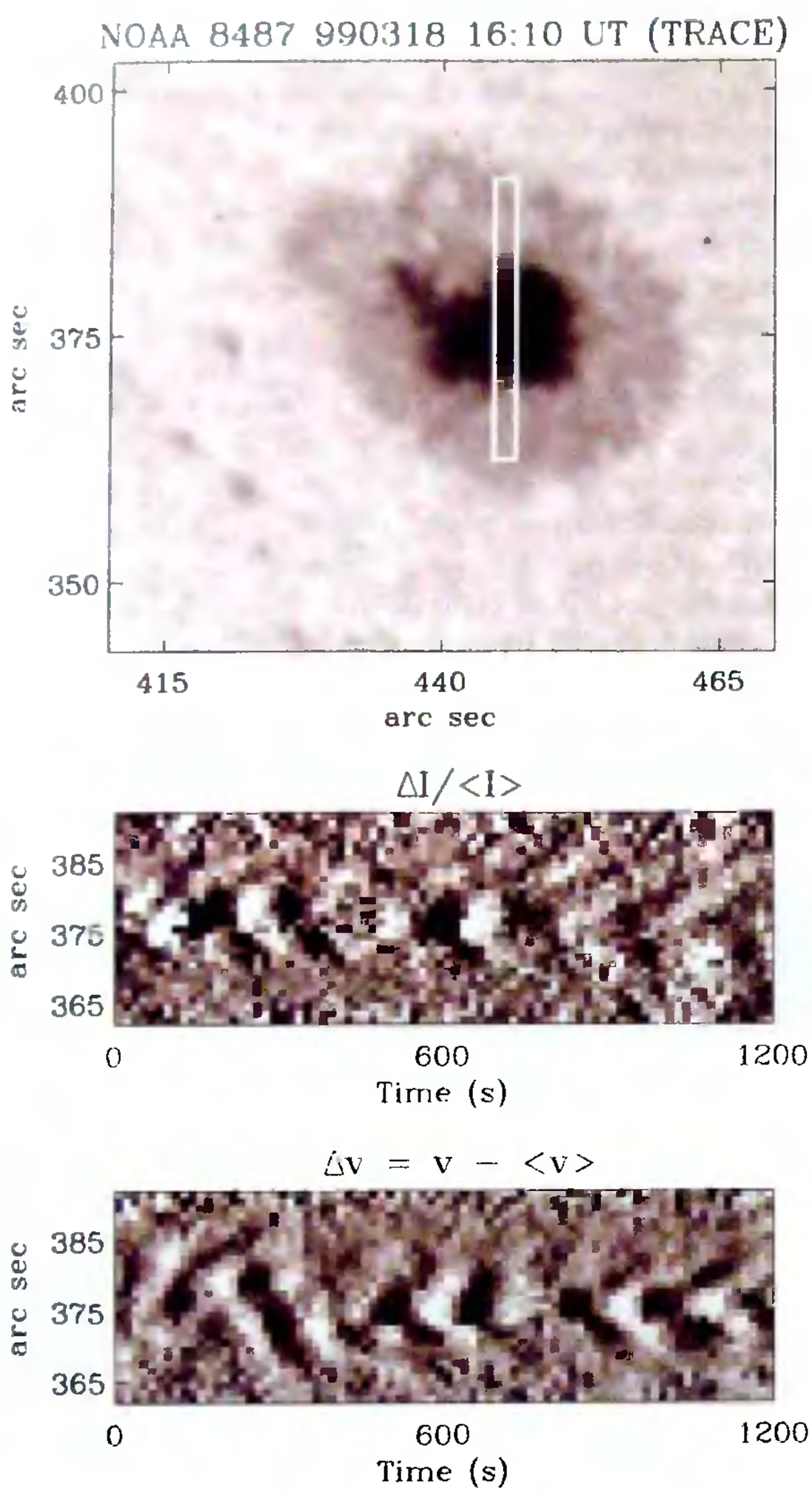

Figure 8. Sunspot oscillations observed with SUMER in the O V (λ629) line. In the upper panel the position of the section of the spectrometer slit analysed is shown with respect to the sunspot of a TRACE image of NOAA 8487 on 18 March 1999. In the lower panels the intensity variations and the line-of-sight velocity along the slit section are displayed (courtesy, N. Brynildsen and the TRACE team).

Sun. Such observations seem to provide the best evidence to date for the existence of bi-directional outflow jets, a fundamental part of the standard magnetic reconnection model. There exists a vast collection of data obtained from the SUMER instrument on the spacecraft *SOHO* and similar bi-directional jets are expected to be seen in the solar atmosphere wherever reconnection takes place. The present and future observations of this kind are likely to provide new clues to a better understanding of how the Sun's magnetic energy feeds its million-degree hot corona and the solar wind.

Sunspot transition region oscillations

The sunspot transition region between the chromosphere and the corona oscillates. This may reveal crucial information about the structure and the physics of sunspots. The first detailed study of the oscillations in the sunspot transition region was presented by Gurman *et al.*[30] mainly based on observations of eight sunspots in the C IV (λ1548) line with the UVSP (Ultraviolet Spectrometer and Polarimeter) instrument on the Solar Maximum Mission. They observed oscillations with periods of 129–173 s, with no signs of shocks and suggested that the oscillations are caused by upward-propagating acoustic waves.

Observations with instruments on *SOHO* have revived the interest for the transition region oscillations. Intensity oscillations in the 2 min range were recently reported[31]. Based on observations with a 15 sec time resolution Fludra[32] has observed 3 min-intensity oscillations and suggested that oscillations occur in sunspot plumes. Combining observations of intensity and line-of-sight velocity oscillations in three transition region lines, Brynildsen *et al.*[33] found that their observations of NOAA 8156 were compatible with the hypothesis that the 3 min oscillations in sunspot transition region are caused by linear, upward-propagating, progressive acoustical waves. This appears to be in conflict with the upward propagating shock waves observed in the sunspot chromosphere[34]. Hence, either the wave amplitude decreases abruptly between the chromosphere and the transition region or considerable difference in the 3 min umbral oscillations exist between different sunspots. Figure 8 shows sunspot oscillations observed with SUMER in the O V (λ629) line. In the upper panel, the position of the spectrometer slit analysed is shown with respect to the sunspot of a TRACE image of NOAA 8487 on 18 March 1999. In the lower panels the intensity variations and the line-of-sight velocity along the slit section are displayed.

Concluding remarks

In conclusion, SUMER results on plasma density and temperature structure, and evidence for hot ions and cool electrons in coronal holes, the 'blue' Sun, observational evidence for magnetic reconnection on the Sun, FIP effect in the corona and sunspot transition region oscillations presented in this article are crucial to a better understanding of how the Sun's magnetic energy feeds its million-degree hot corona and the solar wind. And it will take some time to digest SUMER data to decipher what tricks the Sun is performing!

1. Wilhelm, K., Curdt, W., Marsch, E. *et al.*, *Solar Phys.*, 1995, **162**, 189–231.
2. Wilhelm, K., Lemaire, P., Curdt, W. *et al.*, *Solar Phys.*, 1997, **170**, 75–104.
3. Lemaire, P., Wilhelm, K., Curdt, W. *et al.*, *Solar Phys.*, 1997, **170**, 105–122.
4. Dwivedi, B. N., *Space Sci. Rev.*, 1994, **65**, 289–316.
5. Mason, H. E. and Monsignori-Fossi, B. C., *Astron. Astrophys. Rev.*, 1994, **6**, 123–179.
6. Brown, J. C., Dwivedi, B. N., Almleaky, Y. M., Sweet, P. A., *Astron. Astrophys.*, 1991, **249**, 277–283.
7. McIntosh, S. W., Brown, J. C., Judge, P. G., *Astron. Astrophys.*, 1998, **333**, 333–337.
8. Wilhelm, K., Lemaire, P., Dammasch, I. E., Hollandt, J., Schühle, U., Curdt, W., Kucera, T., Hassler, D. M. and Huber, M. C. E., *Astron. Astrophys.*, 1998, **334**, 685–702.
9. Waldmeier, M., *Die Sonnenkorona I* (1951), *Die Sonnenkorona II* (1957), Birkhäuser Verlag, Basel, Stuttgart.
10. Krieger, A. S., Timothy, A. F. and Roelof, E. C., *Solar Phys.*, 1973, **29**, 505–525.
11. Zirker, J. B. (ed.), *Coronal Holes and High Speed Wind Streams*, Colorado Associated Univ. Press, Boulder, 1977.
12. Dammasch, I. E., Hassler, D. M., Wilhelm, K. and Curdt, W., in *8th SOHO Workshop* (ed. Kaldeich-Schürmann, B.), ESA, SP-446, 1999, in press.
13. Parker, E. N., *Astrophys. J.*, 1958, **128**, 664–676.
14. Wilhelm, K., Marsch, E., Dwivedi, B. N., Hassler, D. M., Lemaire, P., Gabriel, A. H. and Huber, M. C. E., *Astrophys. J.*, 1998, **500**, 1023–1038.
15. Kohl, J. L., Noci, G., Antonucci, E. *et al.*, *Solar Phys.*, 1997, **175**, 613–644.
16. David, C., Gabriel, A. H., Bely-Dubau, F., Fludra, A., Lemaire, P. and Wilhelm, K., *Astron. Astrophys.*, 1998, **336**, L90–L94.
17. Doschek, G. A., Feldman, U. and Bohlin, J. D., *Astrophys. J.*, 1976, **205**, L177–L180.
18. Brekke, P., Hassler, D. M. and Wilhelm, K., *Solar Phys.*, 1997, **175**, 349–374.
19. Chae, J., Yun, H. S. and Poland, A. I., *Astrophys. J. Suppl.*, 1998, **114**, 151–164.
20. Dammasch, I. E., Wilhelm, K., Curdt, W. and Hassler, D. M., *Astron. Astrophys.*, 1999, **346**, 285–294.
21. Hassler, D. M., Dammasch, I. E., Lemaire, P., Brekke, P., Curdt, W., Mason, H. E., Vial, J.-C. and Wilhelm, K., *Science*, 1998, **283**, 810–813.
22. Widing, K. G. and Feldman, U., *Astrophys. J.*, 1993, **416**, 392–397.
23. Sheeley, N. R., *Astrophys. J.*, 1996, **469**, 423–428.
24. Young, P. R. and Mason, H. E., *Solar Phys.*, 1997, **175**, 523–539.
25. Dwivedi, B. N., Curdt, W. and Wilhelm, K., *Astrophys. J.*, 1999, **517**, 516–525.
26. Laming, J. M., Feldman, U., Drake, J. J. and Lemaire, P., *Astrophys. J.*, 1999, **518**, 926–936.
27. Dwivedi, B. N., Curdt, W. and Wilhelm, K., in *8th SOHO Workshop* (ed. Kaldeich-Schürmann, B.), ESA SP-446, 1999 (in press).
28. Dere, K. P., Bartoe, J.-D. F. and Brueckner, G. E., *J. Geophys. Res.*, 1991, **96**, 9399–9407.
29. Innes, D. E., Inhester, B., Axford, W. I. and Wilhelm, K., *Nature*, 1997, **386**, 811–813.
30. Gurman, J. B., Leibacher, J. W., Shine, R. A., Woodgate, B. E. and Henze, W., *Astrophys. J.*, 1982, **253**, 939–948.
31. Rendtel, J., Staude, J., Innes, D. E., Wilhelm, K. and Gurman, J. B., in A Crossroads for European *Solar and Heliospheric Physics* (ed. Harris, R. A.), ESA SP-417, 1998, pp. 277–280.
32. Fludra, A., *Astron. Astrophys.*, 1999, **344**, L75–L78.
33. Brynildsen, N., Leifsen, T., Kjeldseth-Moe, O., Maltby, P. and Wilhelm, K., *Astrophys. J.*, 1999, **511**, L121–L124.
34. Bard, S. and Carlsson, M., in *Fifth SOHO Workshop* (ed. Wilson, A.), ESA SP-404, 1997, pp. 189–191.

ACKNOWLEDGEMENTS. The SUMER project is financially supported by DLR, CNES, NASA, and the ESA PRODEX Programme (Swiss contribution). SUMER is a part of SOHO, the Solar and Heliospheric Observatory, of ESA and NASA. Anita Mohan is supported by the DST, New Delhi, under the young scientist programme.